optica

Multiwavelength polarization-insensitive lenses based on dielectric metasurfaces with meta-molecules: supplementary material

EHSAN ARBABI, AMIR ARBABI, SEYEDEH MAHSA KAMALI, YU HORIE, AND ANDREI FARAON*

T. J. Watson Laboratory of Applied Physics, California Institute of Technology, 1200 E. California Blvd., Pasadena, CA 91125, USA
**Corresponding author: A.F.: faraon@caltech.edu*

Published 10 June 2016

This document contains supplementary methods and materials for "Multiwavelength polarization-insensitive lenses based on dielectric metasurfaces with meta-molecules," http://dx.doi.org/10.1364/optica.3.000628.

http://dx.doi.org/10.1364/optica.3.000628.s001

1. S1. MATERIALS AND METHODS

Simulation

To find the transmission amplitude and phase of a multi-element metasurface, the rigorous coupled wave analysis technique was used [1]. A normally incident plane wave at each wavelength was used as the excitation, and the amplitude and phase of the transmitted wave were extracted. Since the lattice is subwavelength for normal incidence at both wavelengths, only the zeroth order diffracted light is nonzero. This justifies the use of only one transmission value at each wavelength to describe the behavior of meta-atoms. The lattice constant was chosen as 720 nm, and the α-Si posts were 718-nm tall. Refractive indices of 3.56 and 3.43 were assumed for α-Si at 915 nm and 1550 nm, respectively.

The paraxial focal distance of the two lenses were calculated to be 286 μm and 495 μm for the lenses that focus light from the fiber to 400 μm and 1000 μm respectively, by fitting a parabola to the phase profiles of the lenses. For a fitted parabola $y = \alpha x^2$, the paraxial focal distance can be calculated using $f = 2\pi/2\alpha\lambda$. The corresponding numerical apertures can then found to be 0.46 and 0.29 for the two lenses.

The perfect phase mask (that also served as the goal phase profile for the designed devices) was calculated from the illuminating field and the aspherical desired phase profile using the method described in supplementary information of [2]. The illuminating field was calculated by propagating the output fields of single mode fibers at each wavelength using plane wave expansion (PWE) method up to the metasurface layer. The perfect phase mask was then applied to the field, and the result was propagated using the PWE method to the focal point. The diffraction limited FWHM was then calculated from the intensity profile at the focal plane.

Full wave simulation of a full lens was done using finite difference time domain method (FDTD) in MEEP [3]. A lens with a diameter of 75 μm and a focal length of 100 μm was designed with the same method as the fabricated device. The lens focuses the light emitted from a single mode fiber (with mode diameters of 10.4 μm at 1550 nm and 6 μm at 915 nm) placed 150 μm away from a 125 μm thick fused silica substrate (all of the geometrical dimensions were chosen 4 times smaller than the values for the experimentally measured device). The distances to fibers were chosen such that more than 99% of the total power emitted by the fiber passes through the lens aperture. At both wavelengths, the light from the fibers was propagated through air, air-glass interface, and through glass up to a plane about a wavelength before the metasurface using a plane wave expansion (PWE) code. Electric and magnetic field distributions at this plane were used as sources for FDTD simulation of the lenses, and fields were calculated at about a wavelength after the metasurface using MEEP. The PWE code was used again to further propagate these fields to the focal plane and beyond (main text Fig. 4(d)). The focusing efficiencies were calculated by dividing the power in a 20-μm-diameter disk around the focus, to the total power incident on the lens.

Sample fabrication

A 718-nm-thick hydrogenated α-Si layer was deposited on a fused silica substrate using the plasma enhanced chemical vapor deposition (PECVD) technique with a 5% mixture of silane in argon at 200 °C. A Vistec EBPG5000+ electron beam lithogra-

phy system was used to define the metasurface pattern in the ZEP-520A positive resist (∼300 nm, spin coated at 5000 rpm for 1 min). The pattern was developed in a resist developer for 3 minutes (ZED-N50 from Zeon Chemicals). An approximately 100-nm-thick aluminum oxide layer was deposited on the sample using electron beam evaporation, and was lifted off reversing the pattern. The patterned aluminum oxide hard mask was then used to dry etch the α-Si layer in a 3:1 mixture of SF_6 and C_4F_8 plasma. After etching, the mask was removed using a 1:1 solution of ammonium hydroxide and hydrogen peroxide at 80° C.

Measurement procedure

Devices were measured using a fiber placed ∼1100 μm away from the metasurface (500 μm substrate thickness plus 600 μm distance between the fiber and the substrate), and a custom built microscope with ∼100X magnification (Fig. S1). At 915 nm, a fiber coupled semiconductor laser with a single mode fiber with an angled polished connector was used for illumination. Fiber tip angle was adjusted to correct for the angled connector cut. A 100X objective lens (Olympus UMPlanFl, NA=0.95) and a tube lens (Thorlabs AC254-200-B-ML) with a focal distance of 20 cm were used to image intensity at planes of interest to a CCD camera (CoolSNAP K4, Photometrics). A calibration sample with known feature sizes was measured to find the pixel-size transferred to the object plane. The objective was moved with a translation stage to image different planes around the focus. The plotted axial plane intensities are upsampled 2:1 in the axial direction (4 μm adjacent measurement planes distance to 2 μm) to achieve a smoother graph. For focusing efficiency measurement at 915 nm, a 20-μm-diameter pinhole was placed in the focal plane of the metasurface lens to only let the focused light pass through. The pinhole was made by wet etching a 20 μm hole in a thick layer of chrome deposited on a fused silica substrate. A power meter (Thorlabs PM100D with photodetector head Thorlabs S122C) was then used to measure the power after the pinhole, and the output power of the fiber. The efficiency was calculated as the ratio of these two powers. The reported measured efficiency is therefore a lower bound on the actual efficiency as it does not include reflection from the substrate, and two reflections from the two sides of the pinhole glass substrate. A similar setup was used for measurements at 1550: a tunable 1550 nm laser (Photonetics Tunics-Plus) was used with a single mode fiber for illumination. The same 100X objective was used with a 20 cm tube lens (Thorlabs AC254-200-C-ML) to image the intensity in the object plane to a camera (Digital CamIR 1550 by Applied Scintillation Technologies). The camera has a significantly non-uniform sensitivity for different pixels which leads to high noise level of the images captured by the camera (as seen in main text Fig. 4(b)). The nonphysical high frequency noise of the images (noise with frequencies higher than twice the free space propagation constant) was removed numerically to reduce the noise in the axial intensity patterns. The intensity pattern was also upsampled in the axial direction from the actual 4 μm distance between adjacent measurement planes, to 2 μm to achieve a smoother intensity profile. To find the focused power, the focal plane of the lens was imaged using the microscope to a photodetector. A 2 mm iris in the image plane (corresponding to 20 μm in the object plane) was used to limit the light reaching the photodetector. The input power was measured by imaging the fiber facet to the photodetector using the same setup and without the iris. The efficiency was obtained by dividing the focused power by the input power.

2. S2. DISCUSSION OF DEFLECTION EFFICIENCY OF BLAZED GRATINGS DESIGNED WITH THE PROPOSED META-MOLECULE PLATFORM

To understand the reasons behind the low efficiency of the lenses at 915 nm, two double wavelength blazed gratings were designed using the proposed meta-molecule scheme. One grating with a small deflection angle (5 degrees) and another one with a larger angle (20 degrees) were simulated at 915 nm using MEEP, and power loss channels were analyzed in both cases (Fig. S3). Both gratings were chosen to be 2 meta-molecules wide in the y direction, so that periodic boundary conditions in this direction can be used in FDTD. The 5 degree grating is 322 lattice constants long in x direction, while the 20 degree one is 146 lattice constants. The lengths are chosen such that the grating phases at 915 nm and 1550 nm are both almost repeated after the chosen lengths (Fig. S3(a)). An x-polarized plane-wave normally incident from the fused silica side was used as excitation in both simulations, and the transmitted and reflected electric and magnetic field intensities were calculated about a wavelength apart from the meta-molecules. The transmitted fields were further propagated using a plane wave expansion program, and the resulting fields in an area of length 30 μm around the center can be seen in Fig. S3(b and c) for 5 degree and 20 degree gratings, respectively. The field distributions outside of the areas shown here look similar to the ones shown. In both cases, a dominant plane wave propagating in the design direction is observed, along with some distortions. Angular distribution of power in transmission and reflection is analyzed using the Fourier transform of the fields. The resulting power distributions are shown in Fig. S3(d and e) for 5 degrees and 20 degrees, respectively. While the average power transmission of meta-molecules used in both gratings (found from the data in main text Fig. 2(e)) is slightly above 73%, only 36% and 22% of the incident power is directed to 5 and 20 degrees for the corresponding gratings. The actual total transmitted powers are 56% and 50% for the 5 and 20 degree gratings, showing that an additional ∼20% of the power gets reflected as a result of the introduced aperiodicity. Because of the relatively large lattice constant, even a small aperiodicity can result in generation of propagating modes in the substrate, thus the reflection is considerably higher for the gratings than for a perfectly periodic lattice. From the 56% transmitted power in the 5 degree grating, 20% is lost to diffraction to other angles. From Fig. S3(b and c) we can see there are distortions in the transmitted field. These distortions, mainly due to the low transmission amplitude of some of the meta-molecules and their phase errors result in the transmitted power being diffracted to other angles. Besides, it is seen that power loss to other angles both in reflection and transmission is higher for larger grating angles. This is due to the need for finer sampling of the wave front for waves with steeper angles. The lower efficiency for gratings with larger angles results in lower efficiency of lenses with higher numerical apertures which need bending light with larger angles.

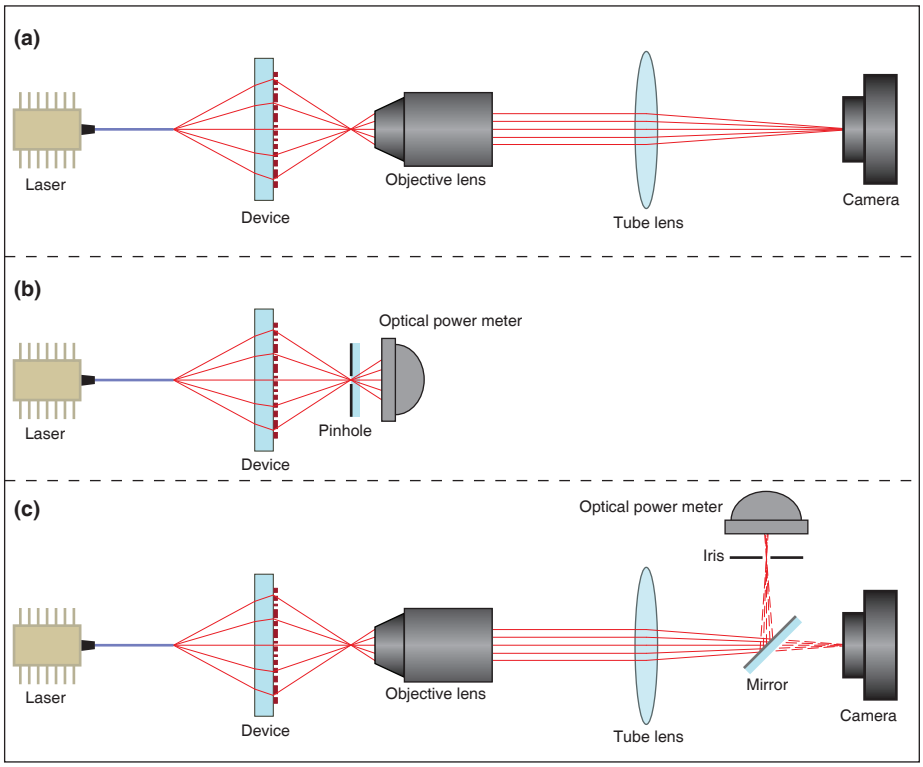

Fig. S1. Measurement setups. (a) The measurement setup used to capture the focus pattern and the intensity distribution in different planes around focus. The laser source, fibers, tube lens, and camera were different in 915 nm and 1550 nm measurements. (b) The measurement setup for measuring the efficiency of the lenses at 915 nm using a 20 μm pinhole in the focal plane. (c), The setup for measuring focusing efficiency of the lens at 1550 nm using a 2 mm iris in the image plane of a $\sim$100X microscope.

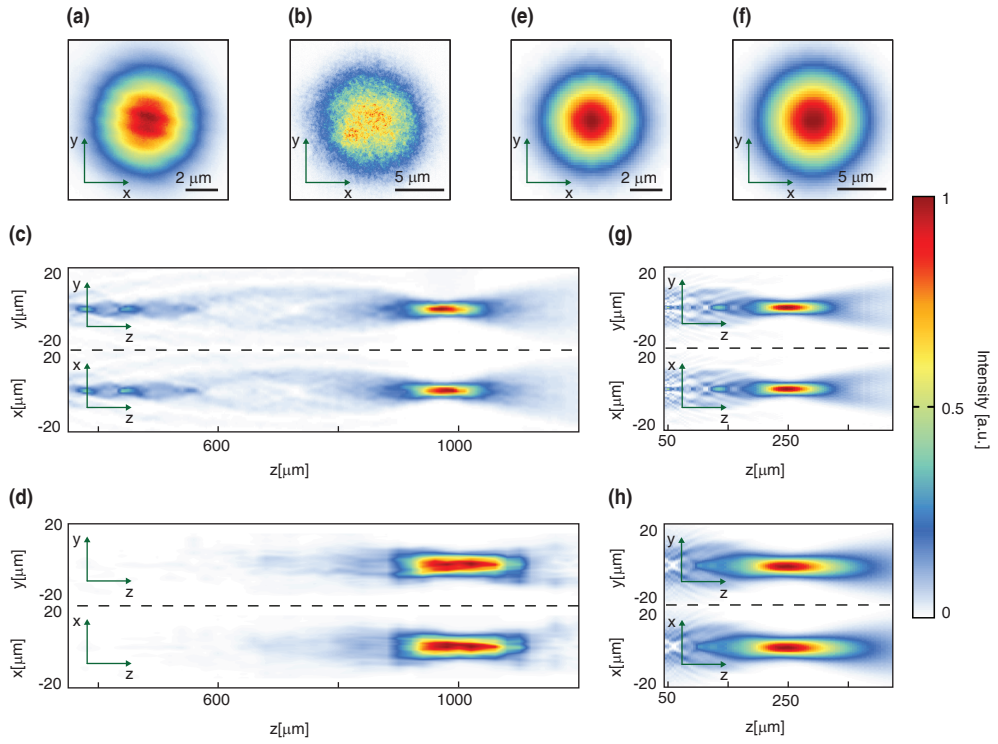

Fig. S2. Measurement and simulation results for the lenses with a lower NA. (a) and (b) Measured intensity in the focal plane of a double wavelength lens (1000 μm focal length, 300 μm diameter) at 915 nm (a) and 1550 nm (b). At 915 nm the lens actually focuses the light 980 μm away from its surface, so the focal spot shown here is imaged at $\approx$ 980 μm away from the surface. The error in focal distance is probably due to the approximation made in the mode diameter of the fiber (see Fig. S1), which affects the focusing distance of a low NA lens more than that of a high NA lens. (c) Intensity measured in the axial planes of the lens for 915 nm. (d) The same axial plots for 1550 nm. (e) and (f) Simulated focal plane intensity of a lens with the same numerical aperture as the one shown in (a–d) but with a dimeter of 75 μm at wavelengths of 915 nm (e), and 1550 nm (f). (g) and (h) Simulated intensity profiles in the axial planes at 915 nm and 1550 nm, respectively, calculated for the same lens described in (e).

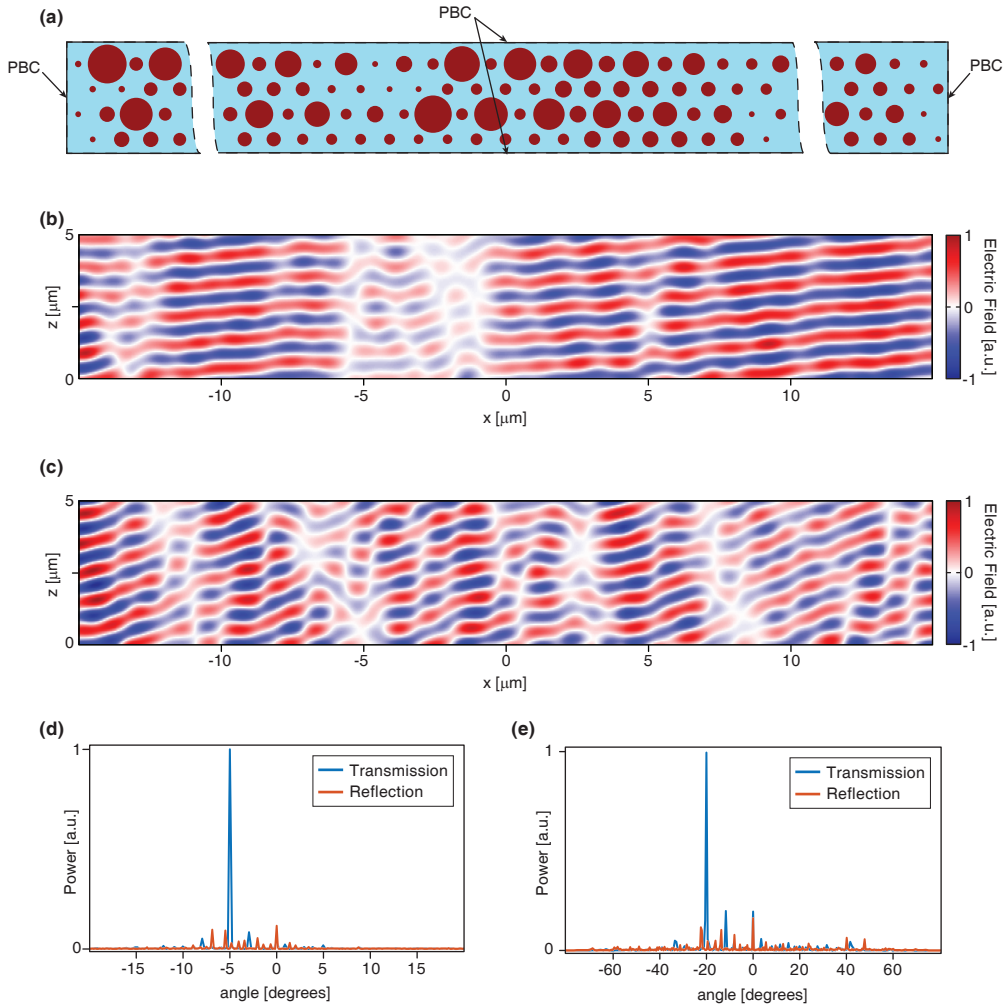

Fig. S3. Double wavelengths blazed gratings based on the proposed meta-molecule design. (a) Schematic of the simulated grating. The 5 degree grating is 322 meta-molecules long, while the 20 degree one is 146 meta-molecules long. Periodic Boundary Conditions (PBC) was used in side boundaries and PML was used to terminate the simulation domain in top and bottom directions. (b) and (c) Real part of the electric field a few wavelengths after the 5 degree (b) and 20 degree (c) gratings. (d) and (e) Distribution of transmitted and reflected power in different angles for the 5 degree (d) and 20 degree (e) gratings.

REFERENCES

1. V. Liu and S. Fan, "S4 : A free electromagnetic solver for layered periodic structures," Comput. Phys. Commun. **183**, 2233–2244 (2012).
2. A. Arbabi, Y. Horie, A. J. Ball, M. Bagheri, and A. Faraon, "Subwavelength-thick lenses with high numerical apertures and large efficiency based on high-contrast transmitarrays," Nat. Commun. **6** (2015).
3. A. F. Oskooi, D. Roundy, M. Ibanescu, P. Bermel, J. D. Joannopoulos, and S. G. Johnson, "Meep: A flexible free-software package for electromagnetic simulations by the fdtd method," Comput. Phys. Commun. **181**, 687–702 (2010).